Eur. Phys. J. D **8**, 395–398 (2000)

THE EUROPEAN PHYSICAL JOURNAL D

EDP Sciences

Temperature behaviour of optical properties of Si^+-implanted SiO_2

J. Valenta[1,a], J. Dian[1], K. Luterová[2], P. Knápek[2], I. Pelant[2], M. Nikl[2], D. Muller[3], J.J. Grob[3], J.-L. Rehspringer[4], and B. Hönerlage[5]

[1] Charles University Prague, Faculty of Mathematics and Physics, Department of Chemical Physics and Optics, Ke Karlovu 3, 12116 Prague, Czech Republic
[2] Institute of Physics, Academy of Sciences of the Czech Republic, Cukrovarnická 10, 16253 Prague, Czech Republic
[3] Laboratoire PHASE[b], 23 rue du Loess, 67037 Strasbourg, France
[4] IPCMS, Groupe des matériaux inorganiques[c], UPL, 23 rue du Loess, 67037 Strasbourg, France
[5] IPCMS, Groupe d'optique non linéaire et d'optoélectronique, 23 rue du Loess, 67037 Strasbourg, France

Received 1st September 1998 and Received in final form 7 September 1999

Abstract. Silicon nanocrystals were prepared by Si^+-ion implantation and subsequent annealing of SiO_2 films thermally grown on a *c*-Si wafer. Different implantation energies (20–150 keV) and doses (7×10^{15}–2×10^{17} cm^{-2}) were used in order to achieve flat implantation profiles (through the thickness of about 100 nm) with a peak concentration of Si atoms of 5, 7, 10 and 15 atomic%. The presence of Si nanocrystals was verified by transmission electron microscopy. The samples exhibit strong visible/IR photoluminescence (PL) with decay time of the order of tens of μs at room temperature. The changes of PL in the range 70–300 K can be well explained by the exciton singlet-triplet splitting model. We show that all PL characteristics (efficiency, dynamics, temperature dependence, excitation spectra) of our Si^+-implanted SiO_2 films bear close resemblance to those of a light-emitting porous Si and therefore we suppose similar PL origin in both materials.

PACS. 78.55.Hx Other solid inorganic materials – 61.46.+w Clusters, nanoparticles, and nanocrystalline materials – 78.45.+h Stimulated emission

Different types of silicon-based nanostructured materials exhibiting efficient photoluminescence (PL) and electroluminescence have been developed in the course of the last decade. One of the most promising methods to prepare Si nanocrystals is the Si^+-ion implantation of SiO_2 [1]. This technique is compatible with the integrated circuit technology and provides nanocrystals with better passivation, durability, long-term stability and controlled size as compared with other Si-based light emitting materials, *e.g.* light-emitting porous silicon.

In this communication we present results obtained on a set of four samples prepared by Si^+-ion implantation of thermally grown SiO_2 layers on a *c*-Si wafer. Time-resolved PL as well as steady-state PL and PL-excitation (PLE) spectra were measured and compared to the red "S band" from typical light-emitting porous Si [2].

Our SiO_2 layers (500 nm thick) were thermally grown on *c*-Si wafers ($\langle 100 \rangle$ *n*-type, resistivity 75 Ωcm) and implanted with Si^+ ions at different energies and different doses in order to obtain layers with different atomic Si content: 5, 7, 10 and 15 at%. To realize a flat implantation profile, a summing of several subsequent implantations was used (see Tab. 1). The total doses vary between $1-2.8 \times 10^{17}$ ions/cm^2. After implantation, the samples were annealed at 1100 °C in a N_2 atmosphere for 4 hours. During this procedure a formation of spherical-like Si nanocrystals in a SiO_2 matrix is supposed [3]. The presence of nanocrystals in our films was evidenced by using the transmission electron microscopy (TEM). Figure 1 presents a high resolution TEM image of one Si nanocrystal (5 nm in diameter) observed in the 10 at% Si^+/SiO_2 layer.

Steady-state PL measurements were performed under excitation with a high-pressure Xe lamp filtered by an excitation monochromator. PL emission was dispersed in an emission monochromator and detected with a photomultiplier connected to a photon counting system. In order to study PL spectra as a function of temperature, the samples were fixed in a temperature variable gas flow cryostat. PL data were corrected for the spectral response of the detection system. A flash Xe-lamp (pulse duration of ~ 2 μs) was used to excite PL in time-resolved PL measurements. The PL decay was detected by a time-correlated photon counting system.

[a] e-mail: valenta@karlov.mff.cuni.cz
[b] UPR 292 du CNRS
[c] UMR 7504 du CNRS

Table 1. Parameters of the multiple Si^+-implantation.

Sample [at% Si]	Implantation energy [keV]	Dose [ions/cm^2]
5	150	6.0×10^{16}
	80	1.9×10^{16}
	45	1.2×10^{16}
	30	7.0×10^{15}
7	150	9.0×10^{16}
	80	2.7×10^{16}
	45	1.6×10^{16}
	20	1.0×10^{16}
10	150	1.3×10^{17}
	70	4.0×10^{16}
	20	1.4×10^{16}
	30	1.3×10^{16}
15	150	2.0×10^{17}
	68	4.3×10^{16}
	43	1.6×10^{16}
	20	1.8×10^{16}

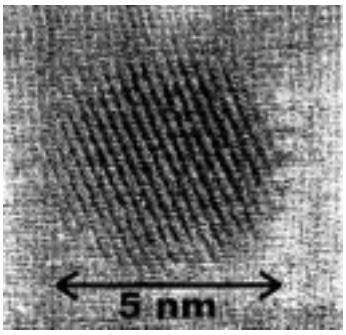

Fig. 1. A TEM high resolution image of a typical Si nanocrystal in the sample containing 10 at% Si. The diameter of the nanocrystal is about 5 nm.

The PL spectra of our samples (solid lines in Fig. 2) consist of one symmetrical red emission band peaked at around 1.6 eV. This emission undergoes a red shift with increasing concentration (total dose) of Si^+-ions. The intensity of this PL band reaches its maximum for the concentration of 7 at% Si. Compared with a typical porous Si PL spectrum (open circles in Fig. 2), PL spectra of Si^+-implanted samples have their maxima at slightly lower energies and are narrower (FWHM is about 0.25 eV).

Is Si^+-implanted SiO_2 film brightly luminescing material? In order to get a rough estimation of the PL emission efficiency, we proceeded as follows. We corrected the PL spectra as well as a PL spectrum of a reference porous Si sample for the amount of the absorbed excitation radiation. The optical absorption of 0.5 μm thick Si^+-implanted SiO_2 film was taken to be equal to the absorption of otherwise identical Si^+-implanted SiO_2 films deposited on a transparent silica substrate (*e.g.* for the 10 at% Si sample

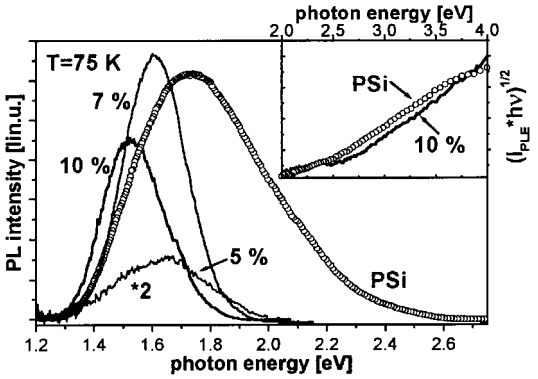

Fig. 2. Photoluminescence spectra ($T = 75$ K, $\lambda_{exc} = 370$ nm) of Si^+-implanted SiO_2 samples with Si concentration of 5, 7 and 10 at% (solid curves in the left-hand side of the figure). The PL spectrum of a typical red luminescing porous Si sample (open dots) is shown for comparison. The PL intensity is corrected for the same number of absorbed photons. The inset shows Tauc plots of PLE spectra ($T = 75$ K) detected at 765 nm for the 10 at% Si sample (full line) and porous Si (open dots).

we measured the absorption of about 9% at 370 nm). The porous Si absorption was estimated to be 90% because the light-emitting porous layer was much thicker – about 20 μm. The spectra in Figure 2 are corrected in this way. One can see that the PL efficiency of Si^+-implanted samples is of the same order as in brightly red luminescing porous Si.

The inset of Figure 2 shows the Tauc plot (*i.e.* plot of $\sqrt{(I_{PLE}h\nu)}$ *vs.* $h\nu$) of PLE spectra of the 10 at% Si sample and of porous Si (detected at 765 nm). The linear shape and close resemblance of both the PLE spectra are remarkable. The intersection of the linear fit of PLE spectra with the x-axis is used to assess the value of the Tauc gap E_g. In our case we have found E_g to be about 2.2 eV. We should stress, however, that the value of E_g (but not the shape of PLE spectra) depends strongly on the correct subtraction of the PLE signal background. The linear absorption behaviour in the Tauc plot means that the indirect optical transitions are responsible for the observed absorption edge [4].

Time-resolved PL experiments exhibit a slow decay of PL in the sub-ms time scale. Decay curves are non-exponential (see Fig. 3). They may be fitted by double exponentials, *e.g.* in the sample 7 at% Si ($\lambda_{PL} = 740$ nm) we found characteristic times of 30 μs and 92 μs. Again, such a slow non-exponential dynamics is typical for porous Si, where it has often been fitted by a stretched exponential $I_{PL}(t) \sim \exp[-(t/\tau)^\beta]$. Using a stretched exponential to fit the PL dynamics in Figure 3 we found parameters: $\tau = 24$ μs, $\beta = 0.67$. This behaviour is usually explained by the dispersive diffusion of photoexcited carriers in localized states in nanocrystal [5,6].

The observation of a peculiar PL temperature behaviour is perhaps the most important results in this paper. The temperature dependence of PL spectra was measured down to liquid nitrogen temperature (from 300 K

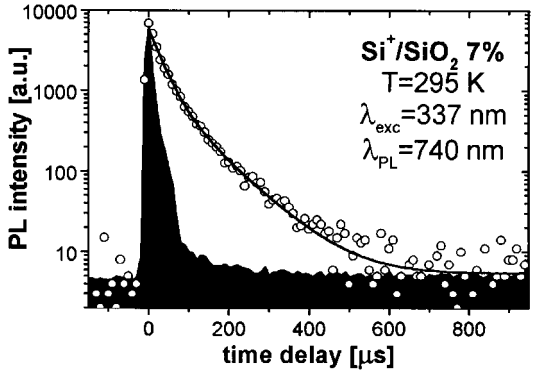

Fig. 3. Microsecond dynamics of PL in the 7 at% Si sample (open dots) at room temperature ($\lambda_{\rm PL} = 740$ nm). The temporal shape of exciting pulse (Xe flash lamp, 337 nm) is shown by a black area graph. PL decay is fitted by a double-exponential with characteristic times of 30 and 92 μs.

to 70 K). In Figure 4, we present the temperature variations of PL spectra of the 7 and 10 at% Si samples (Figs. 4A and 4B, respectively). The salient feature is that PL intensity does not vary monotonously with temperature. It increases with increasing temperature, reaches its maximum between 90 and 130 K and then starts to diminish gradually.

The spectrally integrated PL intensity of the spectra from Figures 4A and 4B are displayed as a function of temperature in the lower part C of Figure 4. The solid lines in Figure 4C are simulations calculated using the model of exciton singlet-triplet exchange splitting in Si nanocrystals which was already used to explain similar temperature behaviour of the S-band in PL of porous Si [7]. This model can be expressed in terms of 4-energy levels E_0, E_1, E_2 and E_3 (see inset in Fig. 4C). The E_0 level represents nanocrystal ground state, the E_1 (E_2) denotes the exciton triplet (singlet) state. The principle attributes of the model are: the $E_1 \rightarrow E_0$ transition is spin forbidden, PL due to optically allowed $E_2 \rightarrow E_0$ transition (*i.e.* $\tau_{20} \ll \tau_{10}$) becomes possible *via* a thermally activated process $E_1 \rightarrow E_2$. However, an excessive increase of temperature already induces non-radiative escape $E_2 \rightarrow E_3$ of the population N_2 from the E_2 level and leads eventually to PL quenching. A steady-state solution of the relevant kinetic equations gives for the PL intensity

$$I_{\rm PL}(T) \approx N_2(T) \approx \frac{g_{12}}{1 + \tau_{20} g_{23} + \tau_{10} g_{12} + \tau_{20}\tau_{10} g_{12} g_{23}},$$

where $g_{ji} = \nu \exp(-E_{ij}/kT)$ denotes the rate of thermally activated transitions $E_j \rightarrow E_i$, ν being a frequency prefactor.

To simulate the temperature dependence of PL we take the mean value from time-resolved PL measurement (60 μs) as the radiative decay time τ_{20}. The theoretical curve of PL temperature dependence from Figure 4A (solid line in Fig. 4C) was obtained for the following set of parameters: $E_{21} = 26$ meV, $E_{32} = 68$ meV, $\tau_{10} = 3$ ms, and $\nu = 1.6 \times 10^5$ s^{-1}. The value of the exchange splitting

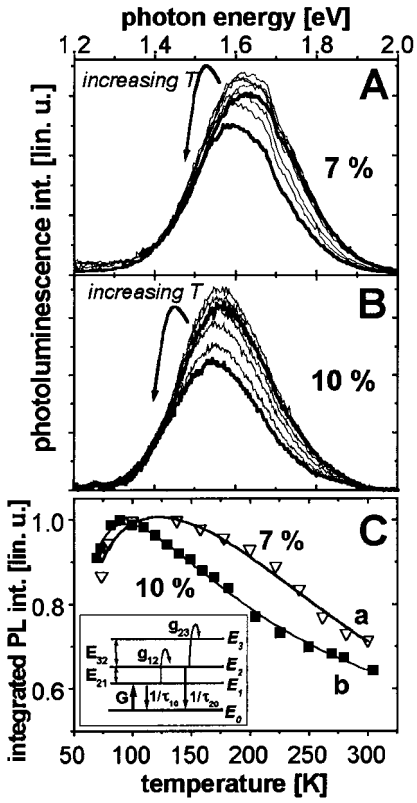

Fig. 4. Temperature dependence of PL for two samples with concentration of 7 and 10 at% Si (part A and B, respectively). The spectra taken at the highest and the lowest temperatures (300 and 70 K) are shown by the bold lines. Part C plots the spectrally integrated PL intensity *vs.* temperature. Lines are calculated using the exciton singlet-triplet splitting model depicted in the inset and described in the text.

energy $E_{21} = 26$ meV is in reasonable agreement with the values quoted for porous Si [8].

It is worth mentioning that the result displayed in Figure 4C clearly demonstrates the ideas behind the exciton singlet-triplet splitting model. Quantum confinement as well as exciton singlet-triplet splitting are larger in smaller nanocrystals. Therefore, in smaller nanocrystals the temperature induced transformation of the triplet excitonic population (energy level E_1) to the higher lying singlet level (E_2) starts at higher temperatures. This is what can really be observed in Figure 4C: the maximum in the temperature dependence for the sample 7 at% Si is at higher temperature than that of the sample 10 at% Si in conformity with Figure 2 (PL band maximum of the sample 7 at% is at higher energy compared with the 10 at% sample, *i.e.* the quantum confinement here is stronger and therefore nanocrystals are smaller in the 7 at% sample).

In conclusion, we prepared Si nanocrystals in thermally grown SiO_2 on *c*-Si substrate by a Si^+-ion implantation and subsequent annealing. Strong visible/IR PL was observed in these samples at temperatures of 70–300 K. PL spectra consist of one symmetrical band which shifts to the red with increasing concentration of Si^+-ions,

i.e. with increasing size of Si nanocrystals. This fact may be explained by weaker quantum confinement effect in nanocrystals of bigger size. The PL efficiency as a function of implantation dose reaches its maximum for the Si concentration of 7 at%. The decrease of PL intensity in samples with higher concentration of Si atoms is probably due to higher probability of non-radiative decay processes. A slow PL dynamics may be approximated by a double-exponential or a stretched exponential decay with characteristic times of the order of tens μs. The non-monotonous temperature dependence of PL can be well explained by the exciton exchange singlet-triplet splitting. Almost all the observed PL characteristics of Si^+-implanted SiO_2 samples – efficiency, dynamics, temperature dependence and excitation spectra – very much resemble those in a typical light-emitting porous Si. It enables us to speculate that the origin of steady-state PL in our Si^+-implanted SiO_2 films is the radiative recombination of electron-hole pairs in Si nanocrystals sized approximately 3–5 nm [9].

This work was supported in part by the GACR No. 202/98/0669 and the GAAVCR No. A1010809 and No. B1112901 grants. Three of us (J.V., P.K., and K.L.) gratefully acknowledge the financial support from the French Government (MENRT) and from NATO linkage Grant HTECH.LG972051.

References

1. T. Shimizu-Iwayama, M. Ohshima, T. Niimi, S. Nakao, K. Saitoh, T. Fujita, N. Itoh, J. Phys. Cond. Matt. **5**, L375 (1993).
2. A.S. Cullis, L.T. Canham, P.D.J. Calcott, J. Appl. Phys. **82**, 909 (1997).
3. S. Guha, M.D. Pace, D.N. Dunn, I.L. Singer, Appl. Phys. Lett. **70**, 1207 (1997).
4. A. Kux, M. Ben Chorin, Phys. Rev. B **51**, 17535 (1995).
5. P. Malý, F. Trojánek, J. Kudrna, A. Hospodková, S. Banáš, V. Kohlová, J. Valenta, I. Pelant, Phys. Rev. B **54**, 7929 (1996).
6. J. Linnros, A. Galeckas, N. Lalic, V. Grivickas, Thin Solid Films **297**, 167 (1997).
7. J.C. Vial *et al.*, in *Microcrystalline Semiconductors: Materials Science and Devices* (MRS Symp., 1993), Vol. 283, p. 241.
8. C. Delerue, G. Allan, M. Lannoo, in *Semiconductors and Semimetals*, edited by D.J. Lockwood (Academic Press, 1998), Vol. 49, p. 253.
9. M.W. Wolkin, J. Jorne, P.M. Fauchet, G. Allan, C. Delerue, Phys. Rev. Lett. **82**, 197 (1999).